

Chlorpyrifos Release Kinetics from Citric Acid Crosslinked Biopolymeric Nanoparticles: A Sustainable Approach

SHEETAL MAAN¹, ANUSHREE JATRANA^{1,*}, VINAY KUMAR², MEENA SINDHU³ and SANCHIT MONDAL¹

¹Department of Chemistry, Chaudhary Charan Singh Haryana Agricultural University, Hisar-125004, India

²Department of Physics, Chaudhary Charan Singh Haryana Agricultural University, Hisar-125004, India

³Department of Microbiology, Chaudhary Charan Singh Haryana Agricultural University, Hisar-125004, India

*Corresponding author: E-mail: anushree@hau.ac.in

Received: 17 September 2023;

Accepted: 28 October 2023;

Published online: 31 October 2023;

AJC-21441

Biopolymer based nanoformulation was synthesized by using microwave assisted nano-precipitation method. The biopolymers consist of chitosan and guar gum were crosslinked using citric acid in order to encapsulate chlorpyrifos pesticide. The successful synthesis of chlorpyrifos containing nano-formulations was thoroughly examined, where the surface morphology examined by using field emission scanning electron microscopy (FE-SEM) has established the loading of chlorpyrifos in the biopolymeric matrix, transmission electron microscopy (TEM) examination revealed the spherical shaped particles of about 234 nm and Fourier-transform infrared spectroscopy (FTIR) analysis has confirmed the crosslinking between two biopolymers through citric acid due to the presence of peaks corresponding to ester linkages at 1730 cm^{-1} . The encapsulation efficiency of chlorpyrifos at pH 7 and $30\text{ }^{\circ}\text{C}$ was around 50%. The successfully synthesized chlorpyrifos loaded biopolymeric nano-formulation were further utilized to study the release behaviour of chlorpyrifos in water and biocompatibility towards soil microbiota. The release of chlorpyrifos was almost 15% slower than conventional chlorpyrifos and the formulation was found biocompatible towards microbiota.

Keywords: Chitosan, Guar gum, Biopolymers, Biocompatibility, Encapsulation efficiency, Nano-formulation, Slow release behaviour.

INTRODUCTION

Agriculture, being the fundamental basis of the worldwide economy, has a multitude of obstacles related to crop pests, diseases and the use of pesticides, which are frequently accompanied by linked issues of toxicity [1]. The excessive and unregulated use of pesticides has further contributed to an alarming rise in incidents of human poisoning posing a significant threat to human health [2]. Nanotechnology offers a viable solution to issues associated with the indiscriminating use of pesticides. The use of nanomaterial-based pesticide formulations can provide green and efficient alternatives for pest management [3]. Nanotechnology permits the regulated release of chemicals in contrast to conventional formulations. This can slow down the rate at which the active agents are depleted in the field as a result of deterioration processes such as evaporation, volatilization and leaching. Small size of nanomaterials aids in proper dissemination on pest surfaces, resulting in more effective

action than conventional pesticides. Aside from their tiny size, nanopesticides do not affect or very slightly harm non-target species [4].

Among many different forms of nanomaterials, biopolymeric nanocarriers are the most promising since they are biocompatible, biodegradable and adaptable for chemical surface modification, allowing for controlled pesticide administration [5]. Herein, we utilized chitosan and guar gum based nanoformulation for slow release of pesticide. Chitosan possess solubility in the acidic media and hydrophilic nature due to the presence of hydroxyl and amine groups and making it suitable as a carrier [6,7]. It can persist over the plant surface for a longer time due to the adhesive nature, also it can form hydrogels and many other modifications due to the presence of deacetylated surfaces [8]. Guar gum is composed of D-mannose backbone having D-galactose at alternate positions and is highly soluble in water only due to the presence of large number of hydroxyl groups. It does not need hot water treatment like

other gums to attain the same level of viscosity in cold water. It has a high degree of water holding capacity due to which it can form hydrogels with other natural polymers which are easily biodegradable, non-toxic, flexible, have biocompatibility and good water retention capacity [9]. Chlorpyrifos (O, O-diethyl O-(3,5,6-trichloro-2-pyridinyl-phosphothiorate)) is a chlorinated organophosphate pesticide. It is a well-known neurotoxic pesticide that targets the central nervous system of pest by preventing the activity of the enzyme acetylcholinesterase. In present study, chitosan and guar gum nanoparticles were synthesized by microwave assisted nano-precipitation method. The synthesized biopolymeric nanoparticles were crosslinked by using citric acid as a green crosslinking agent. The synthesized nanoformulation was used as an encapsulating agent for chlorpyrifos pesticide. The study explores the slow release of pesticide from the chitosan-guar gum nano-formulation under the influence of various conditions.

EXPERIMENTAL

High purity chemicals were used throughout the experiments. Chlorpyrifos (>98% purity) was procured from Sigma-Aldrich, USA and the conventional chlorpyrifos 20% EC (commercial) was procured from local market of Hisar city, India. Chitosan and guar gum (AR) biopolymers were procured from Central Drug House (P) Ltd. India whereas citric acid was procured from Himedia Laboratories Pvt. Ltd., India. Methanol used as non-solvent during synthesis process, was also procured from Central Drug House (P) Ltd., India. Glacial acetic acid used during synthesis of nano-formulation was also procured from Central Drug House (P) Ltd.

Synthesis of chlorpyrifos loaded chitosan and guar gum based nano-formulation: Nano-precipitation assisted by microwaves was used to synthesize the formulation. Using the nano-precipitation technique, first nano-chitosan and nano-guar gum were synthesized. The nano-precipitation method employed was in accordance with Kaur *et al.* [10]. Chitosan (0.25%) and guar gum (0.25%) were dissolved in their respective solvents *i.e.* 0.5% acetic acid solution for chitosan and distilled water for guar gum. Now these solutions were added dropwise to the non-solvent (methanol) with a constant rate flow of about 0.25 mL/min. Citric acid was added as a crosslinker after the resultant solutions were mixed for 1 to 2 h. To further reduce the size of the nano-formulation, microwaves were applied (55 °C for 10 min) to the final mixture. The solution was lyophilized, freeze dried at -80 °C and then kept as a powder. Finally, the resuspended solution of the nano-formulation containing 10 mg of nano-formulation powder added with a predetermined amount of chlorpyrifos was allowed to interact for 24 h. The amount of pesticide loaded was calculated in the terms of encapsulation efficiency. The optimization of encapsulation efficiency was done by varying the concentration of solution carrying chlorpyrifos from 10 ppm to 50 ppm (*i.e.* by adding chlorpyrifos in the range 0.25 mg to 1.2 mg) and by varying time of interaction between nano-formulation and chlorpyrifos *i.e.* from 6 h to 36 h. The resulting solution was centrifuged and the amount of chlorpyrifos in the supernatant was determined by using HPLC. The encapsulation efficiency (EE) was calculated using eqn. 1:

$$EE (\%) = \frac{\text{Total amount of pesticide added} - \text{Unbound pesticide}}{\text{Total amount of pesticide}} \times 100 \quad (1)$$

Characterization: In order to determine the size, stability and interaction between crosslinker and biopolymers, a variety of characterization procedures were used. The FTIR spectrum was recorded by using a Perkin-Elmer Spectrum 3 FTIR spectrometer. The samples were analyzed by using the attenuated total reflectance (ATR) method, in which, the sample was pressed against the high refractive index prism and the totally reflected light was analyzed.

To examine the zeta potential and particle size of the synthesized nano-formulations, Malvern Zetasizer Pro instrument manufactured by Malvern Panalytical, was employed. For the analysis, the samples were first passed through the syringe filter of 0.45 µm pore size. During zeta potential analysis, the samples were filled in a U-shaped cuvette with the help of syringe. A 7610F Plus/JEOL microscope with an accelerating voltage of 20 kV was used for the FE-SEM study. Platinum sputtering was done to make a conductive layer on the surface of the samples at an argon pressure of 10⁻² mbar for 60 s. The TEM analysis was done on a Tecnai 12 G2 microscope, which has a contrast of up to 0.49 nm and a high-end acceleration voltage range of 20 kV to 120 kV. The efficacy of chlorpyrifos encapsulation and its release behaviour was assessed using HPLC. The stationary phase was a C₁₈ column of dimensions 3 × 150 mm and a pore size of 3 µm. The column temperature used was 24 °C and the injection volume was 15 µL. The 90:10 ratio of acetonitrile and water was used as mobile phase, at a flow rate of 0.3 mL/min. A 230 nm was chosen as the detection wavelength for the chlorpyrifos by using a UV detector.

Release behaviour in water: The behaviour of chlorpyrifos released from a nano-formulation under different pH and temperature conditions was studied using distilled water. In this experiment, 20 mL of distilled water with a certain pH and temperature was taken and added with 10 mg of lyophilized nano-formulation powder containing chlorpyrifos. Aliquots (1 mL) of each sample were taken up to 25 days (at intervals of 5 days) and replaced with 1 mL of fresh distilled water with a similar pH, to maintain the volume of the release medium. HPLC was used to analyze the concentrations of the samples that were collected during the experiment.

The temperature was altered as 20, 30 and 40 °C to explore the effect of temperature on release behaviour and the pH was varied as 4, 7 and 10 to study the effect of pH on release behaviour. The release characteristics of conventional formulation and nano-formulation were evaluated. A 0.2 mg (2 mL of 100 ppm) of conventional formulation was added to keep the volume at 20 mL. The following equations were used to compute the cumulative release% during the release experiment [11].

$$\text{Amount of pesticide release (mg/mL)} = \frac{\text{Concentration} \times \text{Bath volume} \times \text{Dilution factor}}{1000} \quad (2)$$

$$\text{Cumulative release (\%)} = \frac{\text{Volume of sample withdrawn (mL)}}{\text{Bath volume}} \times P(t-1) + P_t \quad (3)$$

where, $P(t)$: percentage release at time 't'; $P(t-1)$: percentage release previous to 't'.

$$\text{Release (\%)} = \frac{\text{Amount of pesticide released (mg)}}{\text{Total amount of pesticide in the nanoformulation (mg)}} \times 100 \quad (4)$$

Bio-compatibility towards microbiota: The bio-compatibility of chlorpyrifos containing nano-formulation was studied against some beneficial bacteria of soil and compared with the conventional chlorpyrifos.

Rhizobium and phosphate solubilizing bacteria were used in present work. The inoculation of the sample material was carried out using the well diffusion method and these bacteria were cultured on the YEMA media and nutritional agar media, respectively. In order to conduct the study, 50 μL of the samples were taken. The growth was noticed after 24 h of incubation on these media plates at 30 $^{\circ}\text{C}$.

RESULTS AND DISCUSSION

Encapsulation efficiency: Encapsulation efficiency was used to measure the amount of the active component that was successfully encapsulated within the carrier material. The concentration of the active component in the supernatant was measured using HPLC to evaluate the encapsulation efficiency. The peak at 8.4 min on the chromatogram was associated with the chlorpyrifos, while the other peaks were associated with the solvent. Fig. 1 displays the chromatogram corresponding to chlorpyrifos and solvents.

In Fig. 2, it can be observed that the encapsulation efficiency first increases from 36% to 41.5% with increase in the amount of chlorpyrifos added *i.e.* from 10 to 20 ppm while decreases upto 27.2% with further addition of chlorpyrifos. This is due to limited number of linkages possible in citric acid crosslinked chitosan and guar gum [12]. The encapsu-

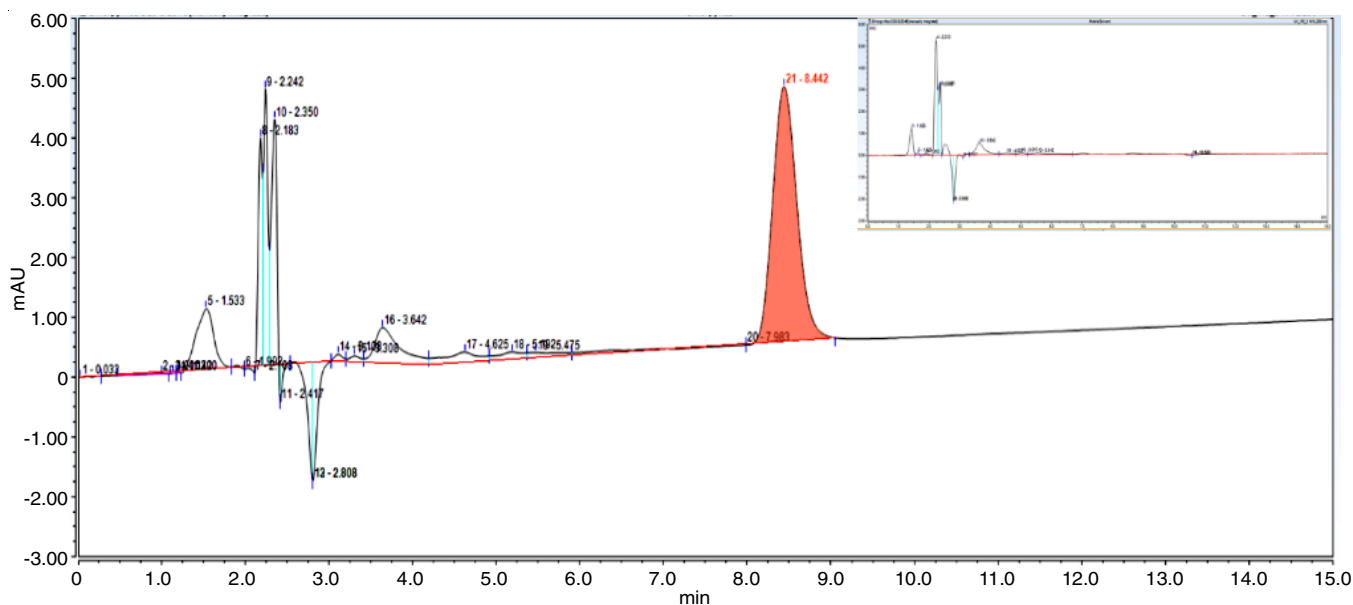


Fig. 1. Chromatogram of chlorpyrifos showing retention time (upper right box is chromatogram for mobile solvent)

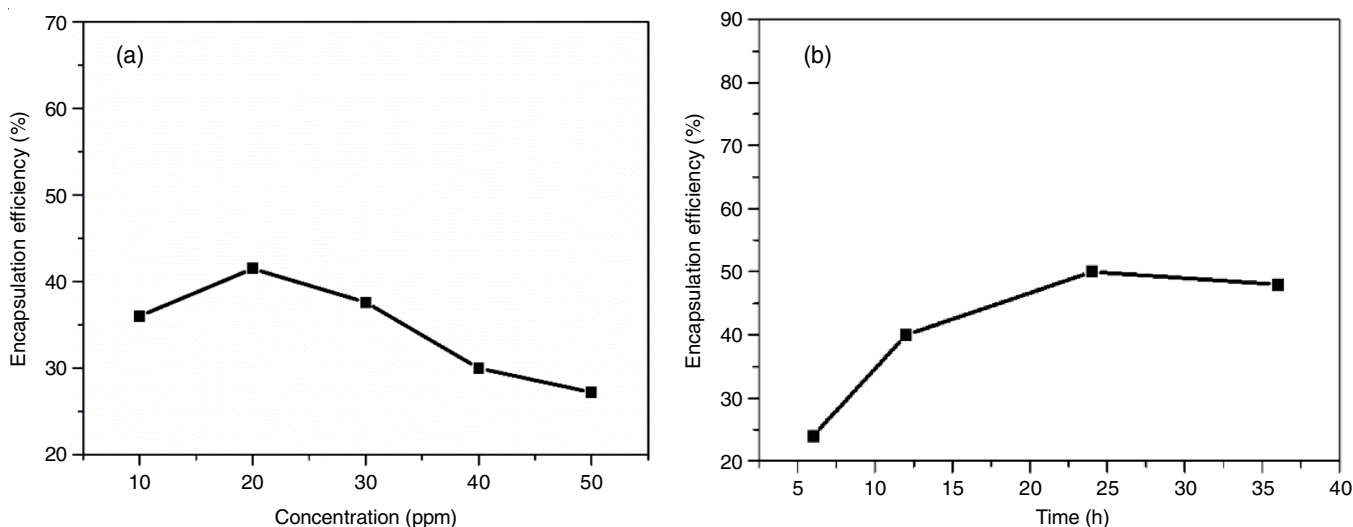


Fig. 2. Variation of encapsulation efficiency of nano-formulation (a) with concentration of chlorpyrifos (b) with interaction time between chlorpyrifos and nano-formulation at optimized concentration

lation efficiency was also found increased from 24% to 49.8% with increase in interaction time from 6 to 24 h and attained equilibrium thereafter. The observed trend in encapsulation efficiency can be related to the progressive creation of a more stable and homogenous encapsulating substance around the pesticide. The encapsulating substance may, however, reach its maximum capacity after a given amount of time and extra contact time may not significantly improve the encapsulation efficiency [13]. Hence, the maximum encapsulation efficiency obtained at optimized conditions was 49.8%.

FT-IR studies: In the FT-IR spectrum of chitosan, the N-H and O-H stretching show a broad peak at 3301 cm^{-1} , while N-H bending vibrations and CH_2 bending vibrations are represented by the peaks between 1300 and 1550 cm^{-1} , C-H stretching is represented by the peak at 2879 cm^{-1} . The peaks near 1050 cm^{-1} , between 1100 and 1150 cm^{-1} and between 620 and 900 cm^{-1} reflect the C-O stretching vibrations, C-N stretching vibrations and N-H wagging vibrations, respectively. Similarly, the FT-IR spectra of guar gum has a broad peak at 3435 cm^{-1} , which corresponds to the O-H stretching frequency, a peak at 2918 cm^{-1} corresponding to the C-H stretching frequency and peaks between 1300 and 1550 cm^{-1} , which correspond to the N-H bending vibrations and CH_2 bending vibrations. The peak for C-O stretching vibration is close to 1050 cm^{-1} . The presence of galactose and mannose 1-4, 1-6 connections are reflected by the peaks at 813 and 870 cm^{-1} , respectively [14].

FTIR spectroscopy confirmed that citric acid established the ester crosslinking between chitosan and guar gum (Fig. 3). The peaks obtained at 1730 cm^{-1} is corresponding to the C=O of ester linkage [15]. After loading of chlorpyrifos, some new interactions between biopolymeric nano-formulation and chlorpyrifos has been established, which resulted into slight shifting and splitting of peak corresponding to ester linkage from 1730 cm^{-1} to 1691 cm^{-1} . The weakening of ester linkage shifts the peak towards lower frequency. The weakening of ester linkage has taken place due to its involvement in interaction with chlorpyrifos ester bonds.

Particle size and zeta potential studies: The sizes of the nano-formulation before and after the loading of chlorpyrifos, were measured using a particle size analyzer (Fig. 4). After adding chlorpyrifos, the size of the nano-formulation increased from 252 nm to 298 nm . It was discovered that the zeta potential for nano-formulation after loading of chlorpyrifos was $+7.3\text{ mV}$. This suggested that the surface of the nano-formulation particles is almost neutral. This might be due to the crosslinking,

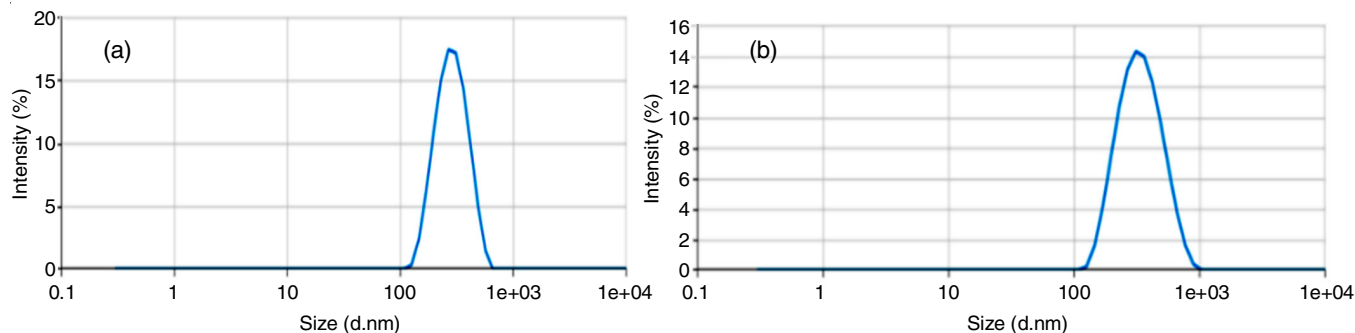


Fig. 4. Particle size distribution of nano-formulation (a) before loading of chlorpyrifos and (b) after loading of chlorpyrifos

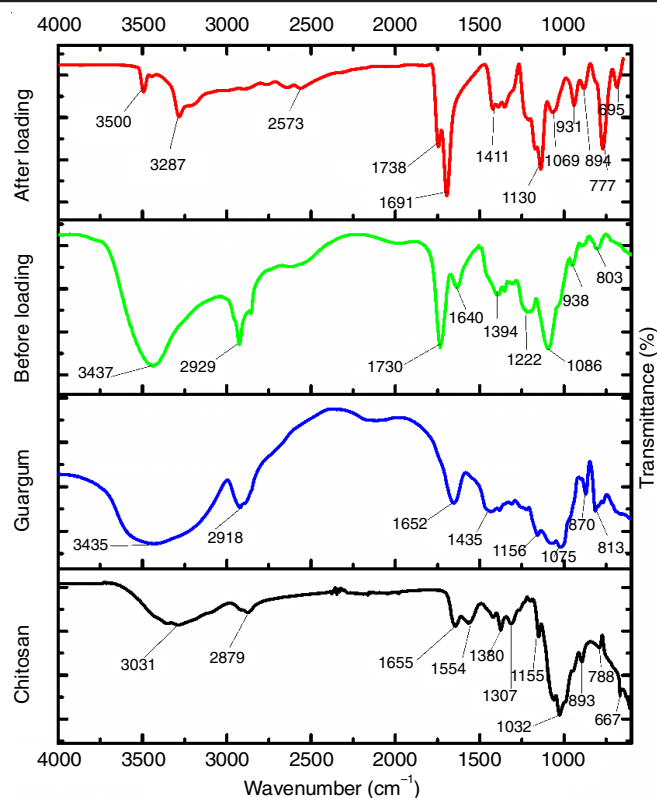


Fig. 3. FTIR spectra of nano-chitosan, nano-guar gum, nano-formulation before loading of chlorpyrifos and nano-formulation after loading of chlorpyrifos

which involve the charged chitosan groups, responsible for surface charge to the nano-formulation particles.

FE-SEM studies: Fig. 5 shows the FE-SEM micrographs of nano-chitosan and nano-guar gum that have been cross-linked with citric acid [16]. The image revealed the uniform and smooth surface of nano formulation. Results obtained were found comparable to the results obtained by Kulkarni *et al.* [17] and Lim *et al.* [18]. As the chlorpyrifos particles have rod like structure [19] and the rod like particles were found entrapped or embedded inside the polymeric matrix (Fig. 5b). This indicated the loading of chlorpyrifos over the blended biopolymer based nano-formulation.

TEM studies: The results corresponding to the TEM analysis are shown in Fig. 6. The images obtained have revealed that the average size of nano-formulation after chlorpyrifos loading was 234 nm . The size obtained from TEM was slightly greater than the size obtained for chlorpyrifos loaded nano-

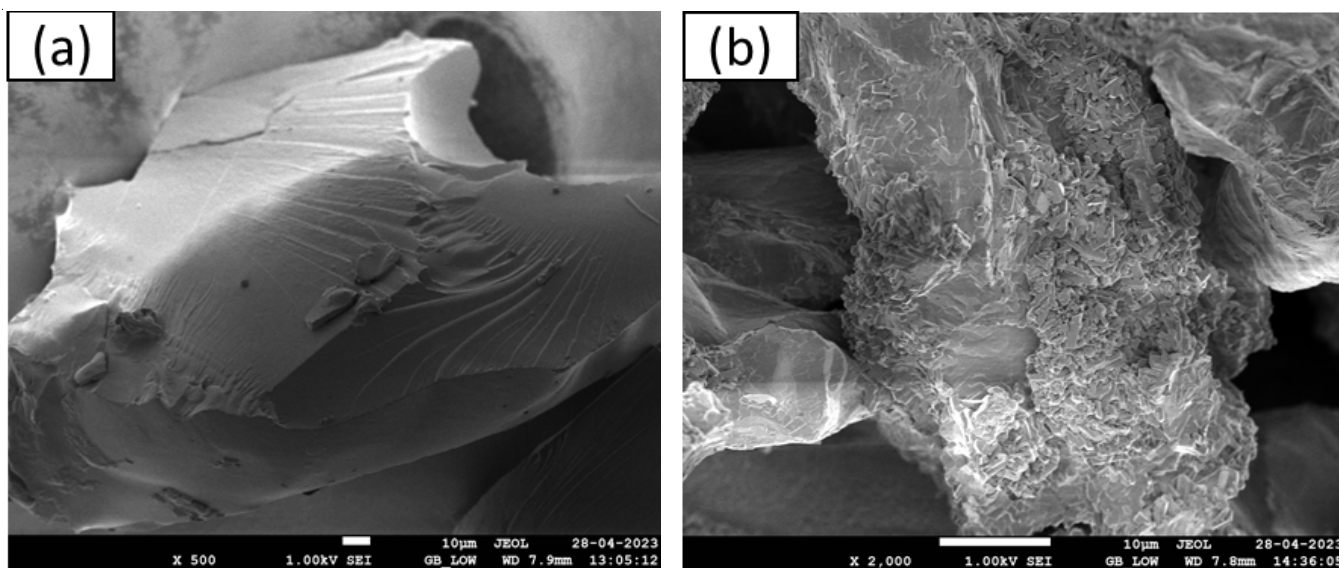


Fig. 5. FE-SEM images of nano-formulation (a) before and (b) after loading of chlorpyrifos

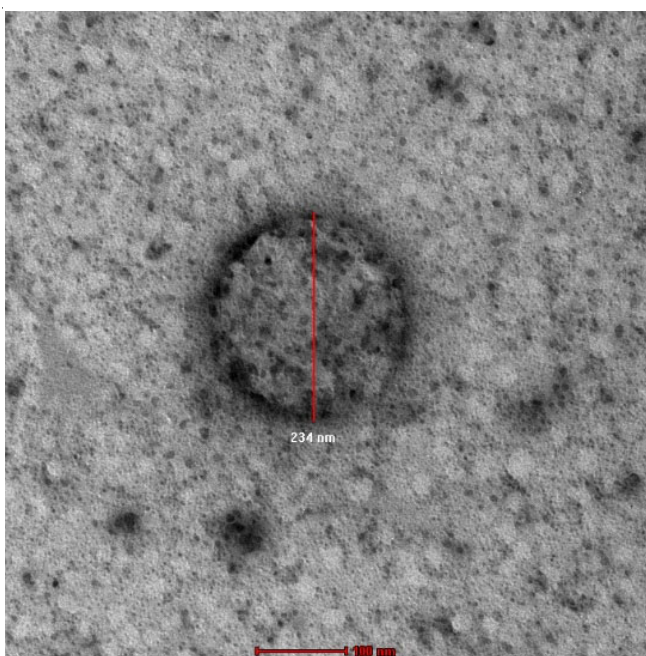


Fig. 6. TEM images of nano-formulation at 100 nm scale

formulation by PSA. This is because the particle size analyzer measures the effective size of a particle as it behaves in a fluid or solution by considering factors like the particle's shape, density and interactions with the surrounding medium [20].

Release behaviour in water

Effect of pH of release medium: The cumulative release percentage increases with almost same rate upto 10 days in different release medium of pH 4, 7 and 10 as shown in Fig. 7a. This is because the ester bonds are feasible to hydrolysis at lower pH as well as basic pH [21]. But the cumulative release percent at pH 4 continues to increase upto 20 days with maximum release of 86.92% on 20th day. In case of pH 7, the cumulative release continues to increase upto 15 days of application with a maximum release of 85.19% on 15th day. Similarly, the cumulative release percent at pH 10 continues to increase only upto 10 days with a maximum release of 83.61% on 10th day of application. From the above data, it was concluded that the cumulative release percent start to decrease after 10 days at pH 10, after 15 days at pH 7 and after 20 days at pH 4. The reason of decreasing cumulative release percent is the degradation of chlorpyrifos released in the medium *i.e.* which is in

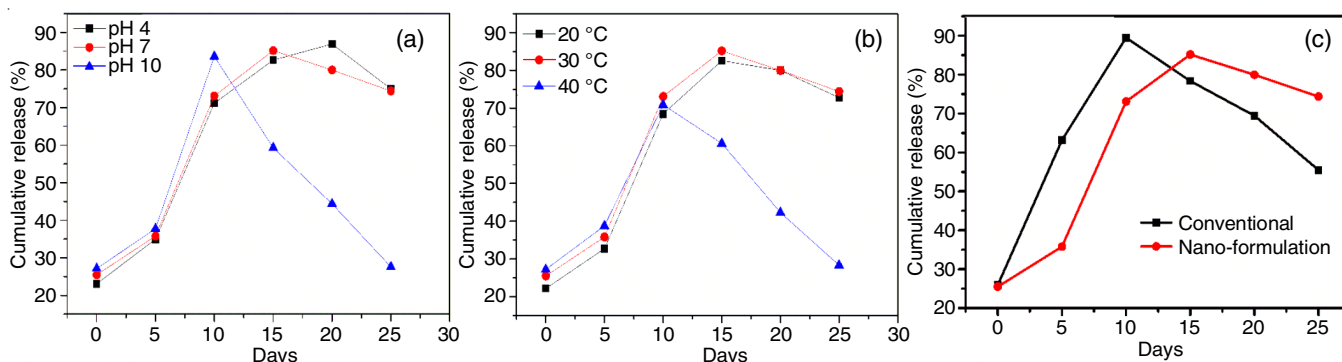


Fig. 7. Effect of (a) pH (b) temperature on cumulative release percent and (c) comparison between cumulative release percent of chlorpyrifos released from conventional formulation and nano-formulation

direct contact with the medium. The degradation occurs at faster rate at higher pH than at lower pH [22].

Effect of temperature of release medium: The cumulative release percentage increases with increase in temperature of release medium and the rate of increase of cumulative release is faster at higher temperature as compare to the lower temperature. The maximum cumulative release percent at 40 °C was 70.88% on 10th of application. In case of 30 °C, the maximum cumulative release percent was 85.19% on 15th of application and in case of 20 °C, the maximum cumulative release percent was 82.59% on 15th day of application. The data revealed that the degradation rate of chlorpyrifos increases with increase in temperature. The degradation of released chlorpyrifos was observed after 15 days at 20 °C and 30 °C and after 10 days at 40 °C, which further resulted into the decrease in cumulative percent release. From Fig. 7b, it can also be established that the cumulative percent release is more at higher temperature, at a particular time period. This can be explained on the basis of the fact that with increase in temperature, diffusion of chlorpyrifos from polymeric matrix to the release medium increases due to increase in the relaxation rate of polymers [23] and also due to increased rate of hydrolysis of ester bonds at higher temperature. So, overall it was found that with increase in temperature, both the degradation rate as well as the release rate have increased [22].

Fig. 7c represents the comparison of release behaviour of chlorpyrifos from the conventional formulation as well as nano-formulation. The graph reveals that the nano-formulation possess greater stability against degradation and releases for longer period of time than conventional formulation *i.e.* upto 15 days. The release of chlorpyrifos from nano-formulation was found almost 15% slower than conventional formulation.

Bio-compatibility towards microbiota: Fig. 8 depicts the antibacterial activity to compare the impact of application of nano-formulated chlorpyrifos and conventional chlorpyrifos against the soil-essential bacteria. This evaluation is crucial for determining if nano-formulated pesticides are appropriate for use on soil microbiota.

The inoculation of sample was done by the well diffusion method. The inhibitory action of sample was analyzed after 24 h of incubation of microbiota in biological oxygen demand incubator at 37 °C. A small inhibition zone around the well was observed in case of conventional formulation due to the

presence of organic solvents, emulsifiers and stabilizers in the conventional formulation (20% EC chlorpyrifos). But there was no inhibitory zone, in case of nano-formulation, which suggests that the biopolymeric formulation is quite compatible with the soil environment in terms of soil-essential bacteria.

Conclusion

The chlorpyrifos loaded biopolymer based nano-formulations of about 234 nm were successfully synthesized by using the citric acid as the crosslinker. The peak obtained at 1730 cm^{-1} corresponding to the ester linkage in the FTIR spectrum, confirms the crosslinking while the roughness of surface in FE-SEM analysis confirmed the loading of chlorpyrifos. The maximum encapsulation efficiency obtained for nano-formulation was about 50%. The nano-formulated chlorpyrifos has shown almost 15% slower release than conventional chlorpyrifos over a period of 15-20 days. These nano-formulations were also found bio-compatible towards soil microbiota. These results suggest the suitability of biopolymer based nano-formulation as a carrier for slow release of chlorpyrifos.

ACKNOWLEDGEMENTS

One of the authors, Mrs. Sheetal acknowledge to CSIR, New Delhi, India for providing SRF (09/303(0311)/2019-EMR-1) fellowship during this research work. The author thanks Department of Biochemistry, Chaudhary Charan Singh Haryana Agricultural University, Hisar, India, for help in the PSA and HPLC analysis.

CONFLICT OF INTEREST

The authors declare that there is no conflict of interests regarding the publication of this article.

REFERENCES

1. N.K. Nandi, A. Vyas, M.J. Akhtar and B. Kumar, *Pestic. Biochem. Physiol.*, **185**, 105138 (2022); <https://doi.org/10.1016/j.pestbp.2022.105138>
2. A. Rehman, M. Farooq, D.J. Lee and K.H.M. Siddique, *Environ. Sci. Pollut. Res. Int.*, **29**, 84076 (2022); <https://doi.org/10.1007/s11356-022-23635-z>
3. E.V.R. Campos, J. Ratko, N. Bidiarani, V. Takeshita and L.F. Fraceto, *ACS Sustain. Chem. Eng.*, **11**, 9900 (2023); <https://doi.org/10.1021/acssuschemeng.3c02282>

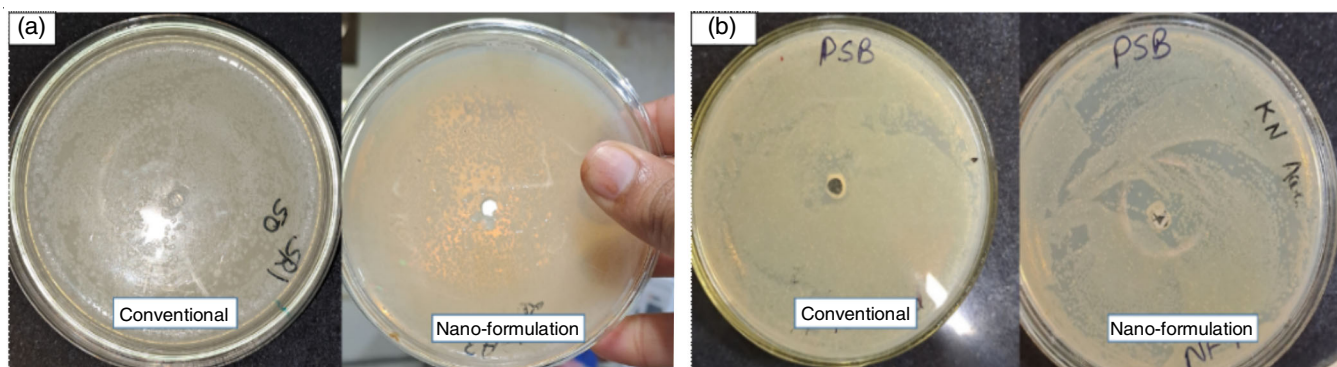


Fig. 8. Antibacterial activity at 24 h against (a) *Rhizobium bacetria* (b) Phosphate solubilizing bacteria

4. T. Hofmann, G.V. Lowry, S. Ghoshal, N. Tufenkji, D. Brambilla, J.R. Dutcher, L.M. Gilbertson, J.P. Giraldo, J.M. Kinsella, M.P. Landry, W. Lovell, R. Naccache, M. Paret, J.A. Pedersen, J.M. Unrine, J.C. White and K.J. Wilkinson, *Nat. Food*, **1**, 416 (2020); <https://doi.org/10.1038/s43016-020-0110-1>
5. V. Raj, C.J. Raorane, J.H. Lee and J. Lee, *ACS Appl. Mater. Interfaces*, **13**, 47354 (2021); <https://doi.org/10.1021/acsami.1c12617>
6. V. Zargar, M. Asghari and A. Dashti, *ChemBioEng Rev.*, **2**, 204 (2015); <https://doi.org/10.1002/cben.201400025>
7. J. Kumirska, M.X. Weinhold, J. Thoming and P. Stepnowski, *Polymers*, **3**, 1875 (2011); <https://doi.org/10.3390/polym3041875>
8. C. Gong, S. Shi, P. Dong, B. Kan, M. Gou, X. Wang, X. Li, F. Luo, X. Zhao, Y. Wei and Z. Qian, *Int. J. Pharm.*, **365**, 89 (2009); <https://doi.org/10.1016/j.ijpharm.2008.08.027>
9. G. Sharma, S. Sharma, A. Kumar, A.H. Al-Muhtaseb, M. Naushad, A.A. Ghfar, G.T. Mola and F.J. Stadler, *Carbohydr. Polym.*, **199**, 534 (2018); <https://doi.org/10.1016/j.carbpol.2018.07.053>
10. M. Kaur, B. Malik, T. Garg, G. Rath and A.K. Goyal, *Drug Deliv.*, **22**, 328 (2015); <https://doi.org/10.3109/10717544.2014.894594>
11. A.R. Chandrasekaran, C.Y. Jia, T. Muniandy, S. Muralidharan, C.S. Theng and S.A. Dhanaraj, *J. Appl. Pharm. Sci.*, **1**, 214 (2011).
12. S. Jiang, C. Qiao, R. Liu, Q. Liu, J. Xu and J. Yao, *Carbohydr. Polym.*, **312**, 120842 (2023); <https://doi.org/10.1016/j.carbpol.2023.120842>
13. A. Roy, S.K. Singh, J. Bajpai and A.K. Bajpai, *Cent. Eur. J. Chem.*, **12**, 453 (2014); <https://doi.org/10.2478/s11532-013-0405-2>
14. D.N. Iqbal, M. Tariq, S.M. Khan, N. Gull, S. Sagar Iqbal, A. Aziz, A. Nazir and M. Iqbal, *Int. J. Biol. Macromol.*, **143**, 546 (2020); <https://doi.org/10.1016/j.ijbiomac.2019.12.043>
15. A.B.S. Agu, P.J.L. Benablo, V.S.D. Mesias and D.P. Penaloza, *J. Chil. Chem. Soc.*, **64**, 4610 (2019); <https://doi.org/10.4067/S0717-97072019000404610>
16. V.G. Bhat, S.S. Narasagoudr, S.P. Masti, R.B. Chougale and Y. Shanbhag, *Int. J. Biol. Macromol.*, **177**, 166 (2021); <https://doi.org/10.1016/j.ijbiomac.2021.02.109>
17. V.H. Kulkarni, P.V. Kulkarni and J. Keshavayya, *J. Appl. Polym. Sci.*, **103**, 211 (2007); <https://doi.org/10.1002/app.25161>
18. H.S. Lim, S. Chae, L. Yan, G. Li, R. Feng, Y. Shin, B.M. Sivakumar, Z. Nie, X. Zhang, Y. Liang, D.J. Bajak, V. Shutthanandan, V. Murugesan, S. Kim and W. Wang, *Energy Mater. Adv.*, **2022**, 9863679 (2023); <https://doi.org/10.34133/2022/9863679>
19. A.M. Bondzic, T.D. Lazarevic Pasti, I.A. Pasti, B.P. Bondzic, M.D. Momcilovic, A. Loosen and T.N. Parac-Vogt, *ACS Appl. Nano Mater.*, **5**, 3312 (2022); <https://doi.org/10.1021/acsnm.1c03863>
20. I. Ban, S. Markus, S. Gyergyek, M. Drogenik, J. Korenak, C. Helix-Nielsen and I. Petrinic, *Nanomaterials*, **9**, 1238 (2019); <https://doi.org/10.3390/nano9091238>
21. C.M. Comisar, S.E. Hunter, A. Walton and P.E. Savage, *Ind. Eng. Chem. Res.*, **47**, 577 (2008); <https://doi.org/10.1021/ie0702882>
22. T.J. Hui, M.M. Ariffin and N.M. Tahir, *Malays. J. Anal. Sci.*, **14**, 50 (2010).
23. A. Roy, J. Bajpai and A.K. Bajpai, *Carbohydr. Polym.*, **76**, 222 (2009); <https://doi.org/10.1016/j.carbpol.2008.10.013>